PRAMANA
— journal of
physics

Supplement to Vol. 41
December 1993
pp. 107–125

Low x structure functions – HERA physics

D K CHOUDHURY
Department of Physics, University of Gauhati, Guwahati 781014, India

1. Introduction

High Energy deep inelastic lepton nucleon scattering (DIS) has been recognised as an important testing ground for the understanding of the structure of matter. Pioneering experiments in this direction started more than twenty years ago. Since then, DIS has been served as the experimental area where QCD is being tested progressively. The advent of HERA [1] has now extended this line of research into new kinematical regions to be accessible in coming years.

2. HERA

HERA is the first electron proton collider built. It is designed to collide 30 GeV electrons or positrons with 820 GeV protons or deuterons. Presently HERA will collide 12 GeV electrons on 480 GeV protons. It is also expected to do experiments with muons and neutrinos.

The complete kinematics of the process is determined by measuring the angle and energy of the scattered lepton, two variables which are directly accessible to the experiments. However, the results are usually presented and interpreted through the variables Q^2, x and y defined below : (Fig.1)

Defining

K_μ = Four-momentum of the incoming electron
K'_μ = Four-momentum of the scattered electron
p_μ = Four-momentum of the incoming proton
s = Available squared energy in the CM system
= $(K+p)^2 \approx 4EE'$

$$Q^2 = -q^2 = -(K-K')^2 \approx 4EE'\cos^2\frac{\theta}{2}, \tag{1}$$

$$x = \frac{Q^2}{2p\cdot q} = \frac{EE'\cos^2\frac{\theta}{2}}{E_p\left(E - E'\sin^2\frac{\theta}{2}\right)}, \tag{2}$$

$$y = \frac{p\cdot q}{p\cdot K} \approx \frac{2p\cdot q}{E} \approx \frac{E - E'\sin^2\frac{\theta}{2}}{E}, \tag{3}$$

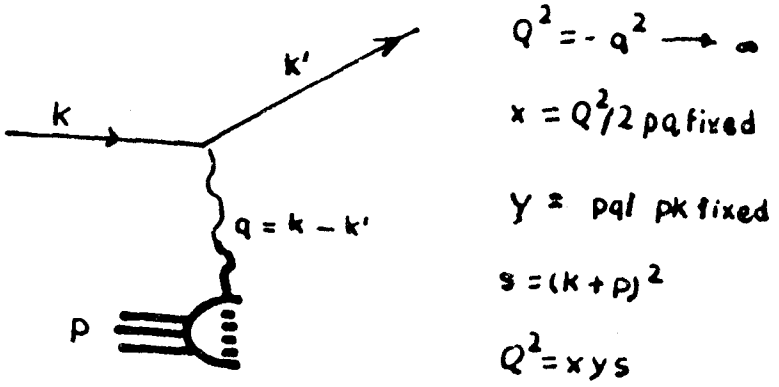

Figure 1. Kinematics of DIS.

where θ = Angle of the scattered lepton measured with respect to the proton direction.

Physically x is the fraction of the proton momentum carried by the struck quark ($0 < x < 1$) while y represents the fraction of the lepton energy transferred to the proton in the proton rest frame. The relation between Q^2. x, y and s is

$$Q^2 \approx x\,y\,s. \tag{4}$$

The accessible range of energy transfer at HERA is

$$200\,\text{GeV} < \nu = \frac{P.Q}{2M} < 52000\,\text{GeV}, \tag{5}$$

while the Q^2 variable reachable at HERA is

$$Q^2 \leq s \approx 10^5\,\text{GeV}^2. \tag{6}$$

In Figure 2 the accessible kinematic x, Q^2 ranges of HERA are shown. Experimental parameters are such that electron detection at low Q^2 and the measurement of highly energetic forward going hadron jets at larger x are excluded. In Figure 3, the accessible kinematical range of HERA compared to fixed target experiments like SLAC and BCDMS [1] is also shown.

Importance is also given to another important machine parameter 'luminosity'. With high luminosity, very intense and compact beams completely passing through each other bring high fluxes of particles very close together and the chance of interaction increases. The design luminosity of HERA is $L = 2 \times 10^{31}\,\text{cm}^{-2}\text{sec}-1$ corresponding to about 1 pb^{-1} per day.

3. Different high energy limits

In order to study low x physics, it is useful to know the connection between the different high energy limits [2]. The Björken [Bj] limit is defined as $Q^2 \to \infty$, $\nu \to \infty$, x finite while the Regge limit is defined as $s \to \infty$, $Q^2 \sim Q_0^2$ fixed (Fig. 4).

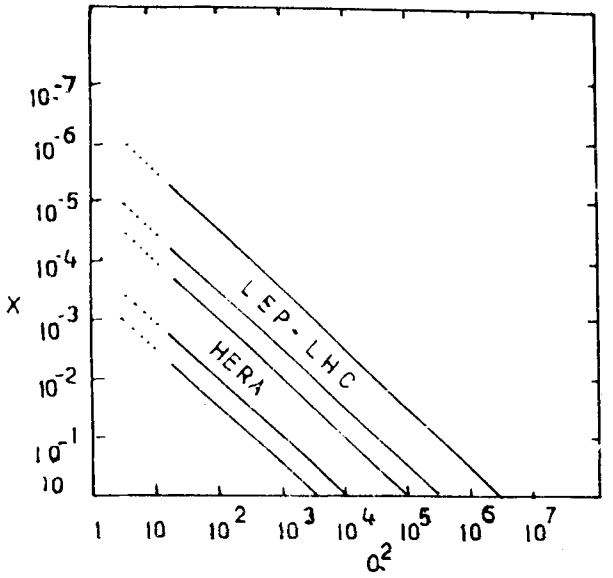

Figure 2. Accessible Kinematics x, Q^2 range at HERA for $Q^2 > 3\,GeV^2$.

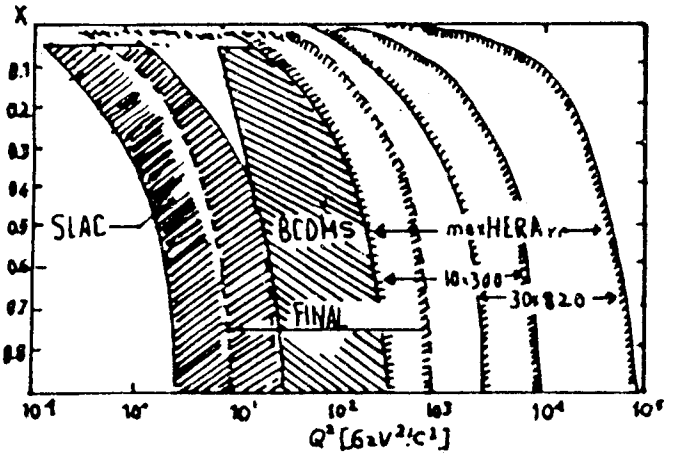

Figure 3. Accessible Kinematic range of HERA compared to fixed target experiments.

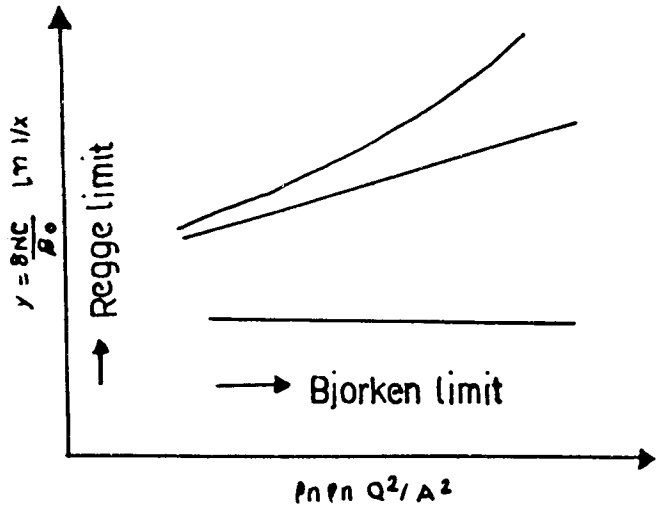

Figure 4. Different High Energy Limits.

For small x DIS physics, one generally uses the following variables :

$$\xi = \ln\ln\frac{Q^2}{\Lambda^2} \qquad \text{and}$$
$$y = \frac{8N_c}{\beta_0}\ln\frac{1}{x} \tag{7}$$

with $\beta_0 = \frac{11}{3}N_c - \frac{2}{3}N_f$, N_c = number of colour, N_f = number of flavour. In Fig. (4), we observe that the small x region, above the Bj limit can be considered as the continuation of the Regge limit towards large Q^2 noting

$$\frac{1}{x} = \frac{2p\cdot q}{Q^2} \approx \frac{s}{Q^2}. \tag{8}$$

Let us now discuss the physics behind these limits. The Bjorken limit (in the horizontal direction of Fig. 4) is the standard region of perturbative QCD. On the other hand, the Regge-limit (in the vertical direction of Fig.4) has a non-perturbative component since scattering with small momentum transfers is dominated by large transverse distances and hence is sensitive to the behaviour of QCD at large distances. In between these two regions, one encounters the small x limit of DIS: it is the region where transition takes place between the region of the perturbative Bj limit and the non-perturbative Regge limit as Q^2 becomes large. Hence, the small x limit of DIS is a testing ground for QCD dynamics: it will indicate how the change-over from the perturbative language of quarks and gluons to that of composite hadrons takes place.

4. Parton picture in small x

Let us now discuss the problem faced by standard QCD. In standard QCD evolutions [3,4], the small-x hehaviour of F_2 is dominated by gluon production and is of

the form [5]

$$xG(x,Q^2) = F_2(x,Q^2) = \frac{\exp\left(\sqrt{2(\xi-\xi_0)y}\right)}{\sqrt{2\pi}\sqrt{2(\xi-\xi_0)}}$$
$$\sim \exp 2\left(\frac{3\alpha_s}{\pi}\ln(Q^2)\ln(\frac{1}{x})\right)^{\frac{1}{2}}, \quad (9)$$

which rises faster than any power of $\ln(1/x) \approx \ln(s/Q^2)$. This gives rises to a critical problem.

The total cross section for the scattering of a virtual photon is related to the structure function as

$$\sigma^{\gamma}_{\text{Total}} = \frac{4\pi^2\alpha}{Q^2}F_2(x,Q^2) \quad (10)$$

and by unitarity, such a cross section cannot grow faster than square of the hadron radius R(s)

$$\sigma^{\gamma}_{\text{Total}} \leq 2\pi R^2(s) \quad (11)$$

where R(s) grows as

$$R(s) = \text{Constant} \cdot \ln s \quad (12)$$

So, somewhere in low x, standard QCD model becomes invalid. One therefore asks: what is wrong in the standard QCD picture and what new physics is to come at low x. The standard QCD evolution is viewed as a cascade of partonic decay processes inside the nucleon: the photon picks up a parton with momentum fraction x and virtuality Q^2. This Q^2 is approximately the transverse momentum squared of the parton. Thus each parton is characterised by the longitudinal momentum component x and the transverse component $\sqrt{Q^2}$. But this struck parton is the final result of a chain of decay processes in the course of which the partons become slower [smaller longitudinal momentum] but of larger virtuality [larger transverse momentum] (Fig. 5). The structure function, is related to the total photon nucleon cross section and hence to the imaginary part of the photon parton Compton scattering. As a result of this one gets the QCD ladder diagram Fig. 6.

Let us discuss this ladder diagram in the transverse plane [2]. Partons at low momentum scale of Q^2 have a rather large transverse size since $R^{\perp 2}_{\text{parton}} \sim \frac{1}{Q^2}$ (Fig. 7a) while those of larger virtuality and low x are thinner (Fig. 7b, 7c). Fig. 7a represent the lower end of the ladder while Fig. (7b, 7c), the upper end. The standard QCD evolution result (9) implies that number of small x partons increases very fast. Eventually they may be so dense that they might even interact.

It is therefore natural to ask if there are also other interaction processes that might balance rise of low x partons or even decrease their density. Indeed, it is pointed out [5] that recombination or annihilation processes might serve this purpose. As a result, in true QCD, the structure function might saturate rather than rise indefinitely (Fig. 8).

Let us see how the new partonic processes can modify QCD evolution. In the standard evolution, a change of parton density (δ_F) is obtained by the splitting of

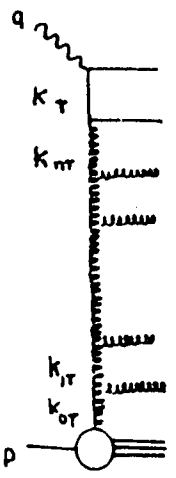

Figure 5. Chain of Decay processes.

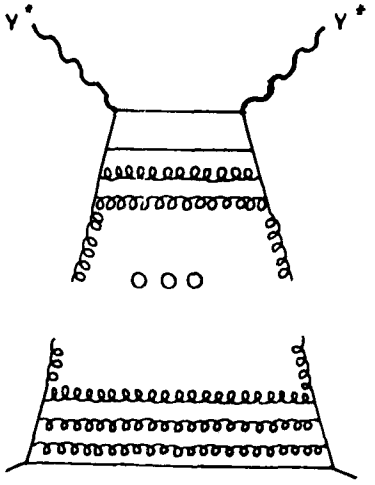

Figure 6. QCD Ladder Diagram describing the standard linear QCD evolution equation of the gluon structure function.

the incoming parton into two outgoing ones. Such a change is proportional to the probability of finding the initial parton

$$\delta_F \propto P \otimes F \tag{13}$$

where P denotes standard splitting functions [4]. Equation (13) yields the linear evolution equation (Fig.9). On the other hand, the recombination process must be proportional to the probability of finding the two initial partons i.e. (Fig. 9).

$$\delta_F \propto V \otimes F^2, \tag{14}$$

which yields non-linear evolution.

Even with these qualitative arguments, one can remark on the strength of such non-linear evolution. If the partons originate from one common "parent" parton (e.g. one valence quark), it is more likely that they have a better chance to recombine than for the case when they come from different valence quarks. Such a recombination process yields the non-planar fan diagram (Fig. 10).

However, before such a non-linear effect takes place, there are suggestions [6] that even within the standard QCD evolution, two important aspects have to be considered at low x:

(a) Higher order terms in the splitting functions of standard evolution need to be taken into account. It is because of such terms that the increase of gluon distribution, Equation (9), may be reduced.

(b) Instead of an exp[ln(1/x)] increase of gluon function in the experimentally accessible range of x, one may even see a $x^{-\frac{1}{2}}$ rise due to the alternative evolution equation, the so called Balitsky-Kuraev-Fadin-Lipatov equation (BKFL) or simply Lipatov equation [7].

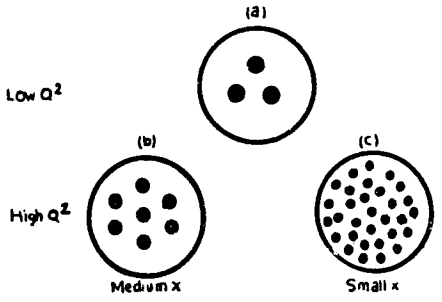

Figure 7. Partons in the transverse plane.

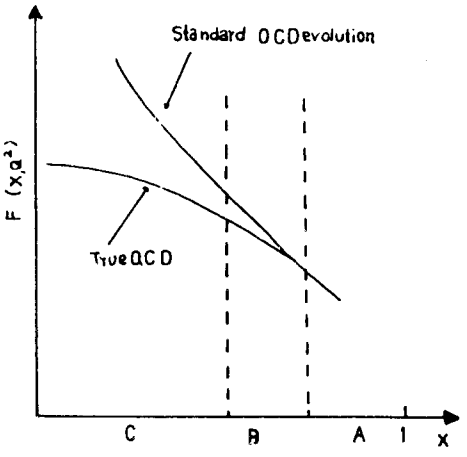

Figure 8. Small X behaviour of the structure function: Standard QCD evolution versus the true QCD evolution. A denotes the perturbative region, B the transition region while C the non-perturbative region.

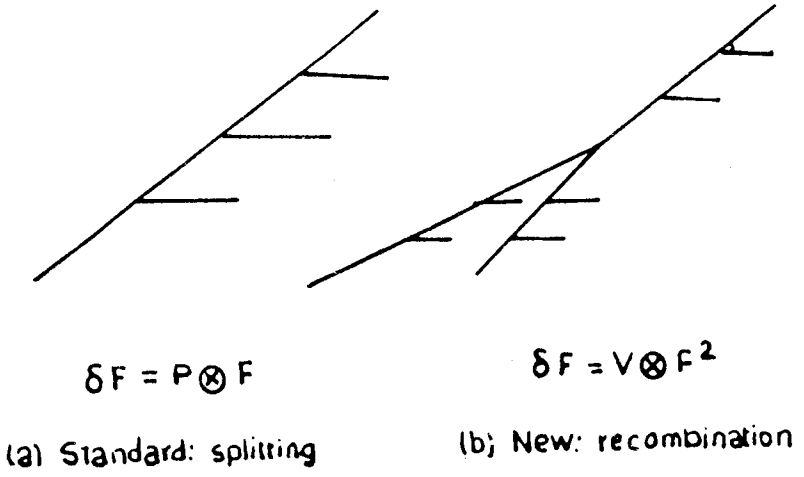

Figure 9. (a) Splitting of partons; (b) Recombination of partons.

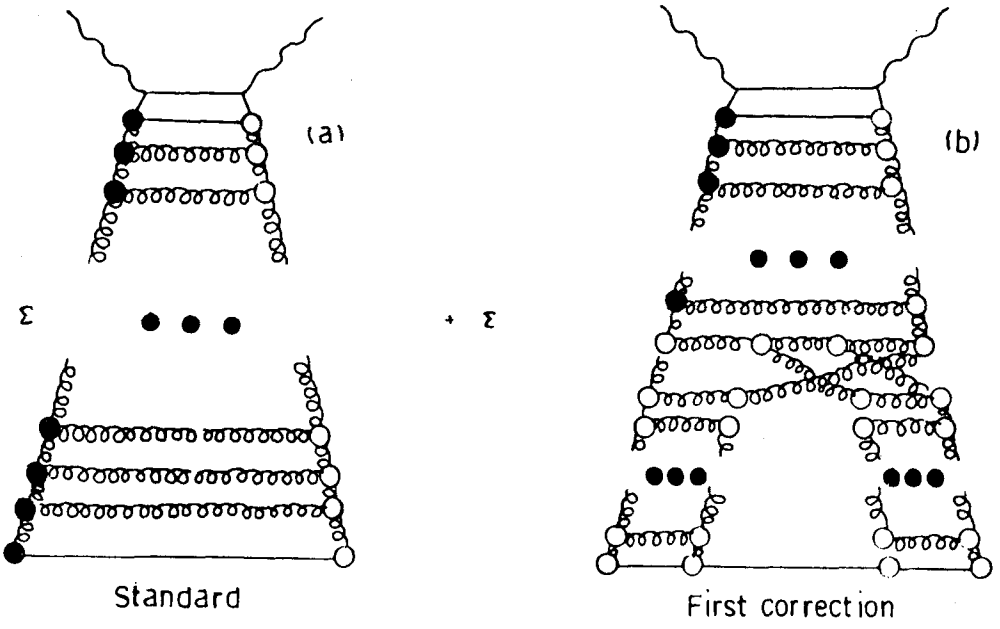

Figure 10. A Fan Diagram versus a standard ladder diagram.

Thus one may conclude that for low x, three equations are of relevance:

(A) Gribov-Lipatov-Altarelli-Parisi Equations (GLAP) with HO splitting function.

(B) Balitsky-Kuraev-Fadin-Lipatov Equation (BFKL)

(C) Non-linear evolution equation or the Gribov-Levin-Ryskin (GLR) Equation.

In the next section, we record these equations.

5. Hot spots

There has been a suggestion [8] that the saturation of partons may actually begin in a non-uniform fashion, Fig. (11). As the simplest example, consider a high density of partons starting to develop first close to the valence quarks whilst other regions inside the nucleon may still remain empty. In such a situation, the structure function would continue to grow with (1/x), but locally saturation might have already reached. Mueller [8] named these regions "hot spots". To measure such non-uniform growth, one has to look for spatial final states which are designed to probe small areas inside the nucleon, to be discussed later.

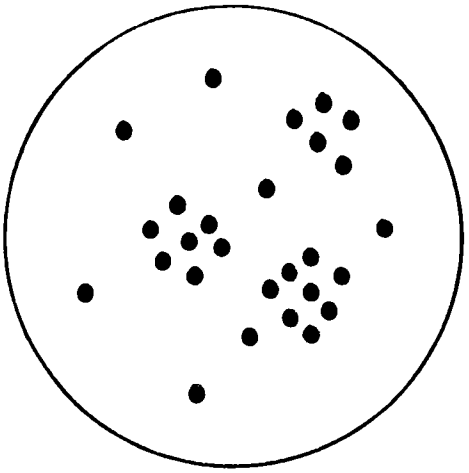

Figure 11. A "Hot spot" in the transverse plane.

6. The evolution equation at low x

6.1. G-L-A-P equations

For gluons, it is

$$\frac{\partial g}{\partial t}(x,Q^2) = \frac{\alpha_s}{2\pi}\left[\Sigma(q+\bar{q})\otimes P_{gq}^{(1)} + g\otimes P_{gg}^{(1)}\right], \tag{15}$$

where $t = \ln\frac{Q^2}{\Lambda^2}$ and

$$g\otimes P = \int_x^1 \frac{dz}{z} g(z,Q^2) P^{(1)}\left(\frac{x}{z}\right), \tag{16}$$

with $P_{ij}^{(1)}$ denoting the LO splitting functions. HO effects in these functions are introduced through the replacements.

$$P_{ij}^{(1)} \rightarrow P_{ij}^{(1)} + \frac{\alpha_s}{2\pi} P_{ij}^{(2)}. \tag{17}$$

The fact that HO 2-loop contributions dampen the LO exponential increase of parton distributions at $x \approx 0$ can be visualised by studying the dominant ($\sim (1/x)$) contributions of these HO functions. For $x \ll 1$, one finds [6]

$$P_{gq} = \frac{8}{3}\frac{1}{x} + \frac{\alpha_s^{\overline{MS}}}{2\pi}\left(-2N_f\frac{40}{27}\frac{1}{x} + \frac{4}{x}\right)$$

and

$$P_{gg} = 6\frac{1}{x} + \frac{\alpha_s^{\overline{MS}}}{2\pi}\left(-2N_f\frac{61}{18}\frac{1}{x}\right). \tag{18}$$

Because of the negative 2-loop contributions in (18), the LO increase of the gluon distribution will be reduced. The sea quark HO term of course contains both positive and negative parts. However for $x \ll 1$, the large $g\otimes P_{gg}$ term should dominate and dampen the LO increase of the sea density as well.

6.2. BKFL equations

This is obtained in the LL (x^{-1}) approximation instead of LL(Q^2). Let us demonstrate it for the n^{th} moment of the gluon function

$$g(n,Q^2) = \int_0^1 dx\, x^n G(x,Q^2). \tag{19}$$

Defining

$$f(n,Q^2) \equiv \frac{\partial g(n,Q^2)}{\partial \ln Q^2}, \tag{20}$$

$$f(n,K^2) = \frac{\partial g(n,Q^2)}{\partial \ln Q^2}\,|_{Q^2=K^2} \qquad (K^2 = \text{finite}),$$

$$f^0(n,K^2) = n^{th} \text{ moment of the input gluon distribution (non} - \text{perturbative)},$$

the BKFL equation reads [7]

$$f(n,K^2) = f^0(n,K^2) + \frac{3\alpha_s}{\pi}\frac{K^2}{n-1}\langle G\rangle, \tag{21}$$

where

$$\langle G\rangle = \int_{K_0^2}^{K^2} \frac{dK'^2}{K'^2}\frac{f(n,K'^2)-f(n,K^2)}{|K'2-K^2|} + \frac{f(n,K^2)}{\sqrt{(2K'^2+K^2)^2-4K^2K'^2}}. \tag{22}$$

Equation (9) based on GLAP evolution does not take into account all the leading terms in the small x limit. It neglects the terms which contain the leading power of $\ln(1/x)$ but are not accompanied by leading powers of $\ln(Q^2)$. Taking into account these leading $\ln(1/x)$ terms, the BKFL equation is obtained. Under the assumption that α_s is not running, it has a simple solution

$$x\,g(n,Q^2) \sim x^{-\alpha_P+1} \tag{23}$$

with

$$\alpha_P - 1 = \frac{12\alpha_s}{\pi}\ln 2. \tag{24}$$

α_P is called the intercept of the socalled bare QCD Pomeron, Lipatov Pomeron or simply Perturbative Pomeron [9].

For a typical value of $\alpha_s \sim 0.2$, $\alpha_P - 1 \sim 0.5$ and so

$$\lim_{x\to 0} x\,g(x,Q^2) \sim x^{-\frac{1}{2}} \tag{25}$$

Clearly, the growth in Equation (25) cannot go on indefinitely with decreasing x, since eventually the density of gluons will become so large that they can no longer be treated as free partons leading to recombination processes. However, there may be an "intermediate" region of x with $x \sim 10^{-3}$ where these shadowing or recombination effects are expected to be small and where the rapid "Lipatov

Growth" should be evident. The possibility of testing such scenarios at HERA will be discussed later.

6.3. GLR equation

In the approximation where only leading power of $\ln Q^2$ and $\ln(1/x)$ are kept (DLA approximation), compact forms of GLR equations are shown in the recent literature [2, 6]. A further approximation is that the coupling of any $n \geq 2$ ladder to the hadron is proportional to the n^{th} power of a single ladder. As a result, the probability of finding two gluons (at low momentum Q_0^2) with momentum fractions x_1, and x_2 is proportional to $g(x_1, Q_0^2) \cdot g(x_2, Q^2)$. This leads to a non-linear integro-differential equation for the structure function [2,3] :

$$\begin{aligned} F(y,\xi) &= X\,g(y,\xi)\,, \\ \frac{\partial F(y,\xi)}{\partial \xi} &= \frac{1}{2}\int_0^y dy' F(y',\xi)\left[1 - 2C\exp\left\{-e^{-\xi} - \xi\right\} F(y',\xi)\right], \end{aligned} \tag{26}$$

with C representing the coupling strength.

A more accurate form of the GLR equation reads

$$\begin{aligned} \frac{\partial \Phi(n,Q^2)}{\partial \ln(1/x)} &= \int \hat{K}(q^2,q'^2)\Phi(x,q'^2)\frac{4N_f\alpha_s(q'^2)}{4\pi}\alpha q'^2 \\ &\quad -\frac{1}{4\pi R^2}\left(\frac{\alpha_s(q^2)}{4\pi}\right)^2 V\cdot\Phi^2(x,Q^2), \end{aligned} \tag{27}$$

where $\Phi = \frac{\partial F}{\partial Q^2}$, R denotes the transverse radius of the hadron and V stands for the triple ladder vertex. However unlike fot the GLAP or BKFL equation, approximate analytic solutions of (26) and (27) are not available.

6.4. Parton distributions at low x

As a direct consequence of the above theories, non-perturbative parton distributions have also undergone radical change. The traditional form of the gluon distribution was

$$x\,g(x,Q_0^2) \sim \text{constant as } x \to 0. \tag{28}$$

Inspired by the Lipatov singularity, the input gluon distribution is also now constructed with a singular form

$$x\,g(x,Q^2) = C(x)x^{-\frac{1}{2}}. \tag{29}$$

Several authors [10–12] have made explicit parametrizationsof this form. We only cite simple one of Kwiecinski et al [10] at $Q_0^2 = 4\,GeV^2$:

$$x\,g(x,Q^2) = 0.265x^{-\frac{1}{2}}(1+20x)(1-x)^{5.5}, \tag{30}$$

$$\begin{aligned} x\,S(x,Q^2) &= 2(\bar{u}+\bar{d}+\bar{s}) \\ &= 0.168x^{-\frac{1}{2}}(1+27.4x^{\frac{1}{2}}+263x)(1-x)^{9.9}. \end{aligned} \tag{31}$$

There is also one set of parametrizations of Morphin and Tung [11] with $xg(x) \sim x^{-\frac{1}{3}}$ and another one of Gluck, Reya and Vogt [12].

6.5. Non-perturbative evolution at small x

When the transverse momentum of an exchanged quark or gluon (K^2) is much larger than 1 GeV^2 (say), the quark and gluon propagators take their perturbative forms. But for small K^2, non-perturbative effects might dominate. Basing on these arguments, Donnachie and Landshoff [13, 14] parametrised small Q^2 SLAC and EMC data with following parametrizations:

$$F_2^{\text{Valence}} = 1.33x^{0.56}(1-x)^3\left(\frac{Q^2}{Q^2+0.85}\right)^{0.44}, \tag{32}$$

$$F_2^{\text{Non-valence}} = 0.17x^{-0.08}(1-x)^5\left(\frac{Q^2}{Q^2+0.36}\right)^{1.08}. \tag{33}$$

Recently [15], some more work has been done on this front with recent low x, low Q^2 EMC data [16] applying the approximate solutions [17] of the GLAP equation at low x.

7. Tests of theories at HERA

7.1. GLAP versus GLR effects

In recent years, quantitative studies of non-linear effects have been made [10, 18, 19]. Fig. 12 shows representative results [19] of such studies. The absolute size in the small x region depends on the inputs chosen and the size of the triple ladder coupling strength

$$C = 9K\alpha_s^2(Q^2)/2R^2, \tag{34}$$

with $K \sim O(1)$. In the Figure 12, we show the x-dependence of gluon distributions at $Q^2 = 10$ and 10^4 GeV^2 [19] as derived from (26). The dashed curves represent C corresponding to the use of $R = 1$ GeV^{-1} and dotted ones to C/10. In each case, the lower curves belong to the ELHQ [20] flat input $xg \sim$ constant as $x \to 0$, whereas the upper curves belong to the steeper MT input [11] at $Q_0^2 = 4\,GeV^2$. The solid curves, on the other hand, refer to the linear LO evolution without the non-linear term. As pointed out earlier, non-linear effects have reduced the gluon distribution, although the quantitative value is sensitive to the hadronic radius R as well as other inputs.

One also asks the question [6] if the GLAP equation with HO splitting functions also simulates the similar reduction. In Fig. 13, we show the x-dependence for $xg(x,Q^2)$ based on LO and HO linear evolutions as reported by Gluck, Reya and Vogt [12] together with the non-linear result of Fig. 12 with the ELHQ input [20]. As can be seen, the non-linear term of (27) can reduce, through an appropriate value of R^{-1}, the LO increase by the same amount [6] as does the linear HO term. We note that the HO predictions cannot be changed substantially because there is no free parameter. On the other hand, this is not for the non-linear effect. Reya [6] comments that a steeper input for xg (x), possibly even slightly steeper than MT input [11], will yield results which practically coincide with the ones obtained from the linear HO evolutions shown in Fig. 13.

Apart from these ambiguities, deviations from the linear LO evolution become visible already at $x \sim 10^{-2}$ in both cases as can be seen from Fig. 13. One can

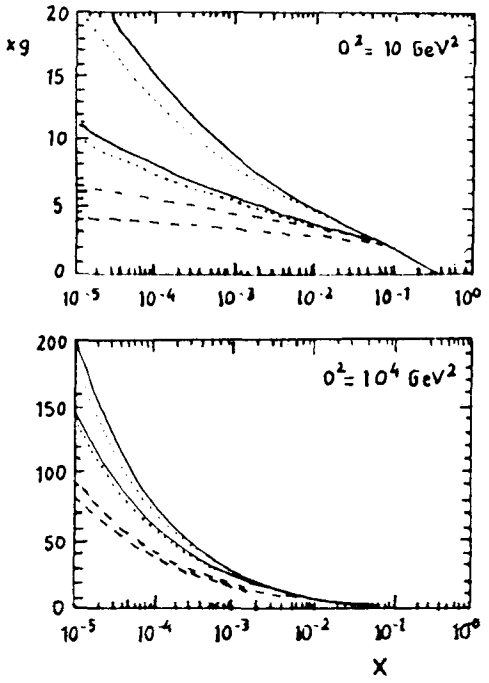

Figure 12. The X dependence of gluon distributions at $Q^2 = 10$ and 10^4 GeV^2. The full curves refer to the linear LO evolution and the dashed ones to the non-linear case.

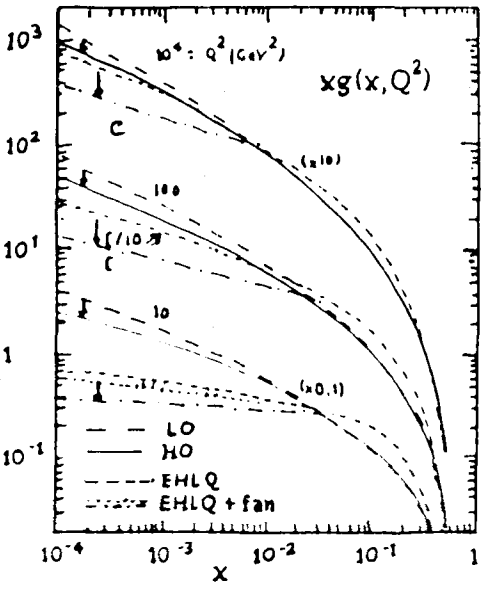

Figure 13. Comparison of the predictions for the reduction of the LO increase of the gluon distribution by HO and non-linear effects.

therefore conclude that it will be very hard to distinguish experimentally between the two cases. The best way to distinguish between the two is the comparison of evolution in Q^2: linear and non-linear evolution predict different Q^2 dependences. In order to extract this from data, we need a range of Q^2 as large as possible. Whether HERA will satisfy this requirement is not yet clear.

7.2. Probing the Lipatov singular small x behaviour at HERA

As pointed out earlier, in connection with (23), a characteristic expectation of perturbative QCD in the small x regime is the $x^{-\lambda}$ behaviour which results from BKFL equation. One consequence is that the gluon (and sea quark) distributions are expected to behave as

$$xG(xq_{sea}) \sim x^{-\lambda}, \tag{35}$$

where $\lambda \sim 12\pi^{-1}\alpha_s \ln 2$

In common lore, λ is identified as

$$\lambda = \alpha_p - 1, \tag{36}$$

where α_p is the intercept of the so-called "Lipatov Pomeron" and, since $\alpha_p - 1 \sim 0.5$ for a typical $\alpha_s \sim 0.2$, we should expect to see a spectacular growth, namely (25). We have already mentioned that there is an "intermediate" region of x, with $x \sim 10^{-3}$, where these shadowing or recombination effects are expected to be small and where the rapid "Lipatov" growth of (25) should be evident.

So far, experiments have not been able to probe down to such small x values (at least for Q^2 large enough to be in the perturbative region) and so no confirmation of the Lipatov Pomeron exists yet. Indeed, there has been doubt in the recent literature [21] whether it will be possible to separate such perturbative behaviour from the non-perturbative one. Measurements of the deep inelastic structure functions $F_1(x,Q^2)$ and $F_2(x,Q^2)$ at HERA can probe $G(x, Q^2)$ and $\bar{q}(x,Q^2)$ respectively in this region of x, but over a limited range of Q^2. The comparison of the experimentally determined parton distributions with the QCD predictions is complicated by the need to put some starting parton distribution (such as their x behaviour at $Q_0^2 = 4\ GeV^2$) in the QCD calculation. Thus, if a steep behaviour is observed at small x like (25), one cannot guarantee that it is not a non-perturbative effect due to input parton distributions.

On the other hand, a study of the Q^2 dependence would also appear to be of little help. The steep behaviour with decreasing x that is generated by the Lipatov equation is stable to evolution in Q^2. Moreover, the Q^2 dependence arising from the Lipatov equation is similar to that given by GLAP evolution [3, 4]. Finally, only a limited range of Q^2 is accessible at HERA for small values of x.

It is clearly desirable to look for experiments which can focus on the small X behaviour of QCD (rather than its Q^2 behaviour) and which do not depend on some input x distributions. An intriguing proposal has been made by Mueller [8, 22] which is nowadays termed as a landmark measurement at HERA. The idea is to study deep inelastic (x, Q^2) events which contain an identified jet (x_j, K_T^2) where $x \ll x_j$ and $Q^2 \sim K_T^2$. Here $x_j p$ and K_T are the longitudinal and transverse momenta of the jet in a collinear proton-photon frame in which the proton momentum is large. The process is illustrated in Fig. 14 where the jet arises from parton (quark or gluon) a. The longitudinal momentum fraction x_j carried by the jet is chosen

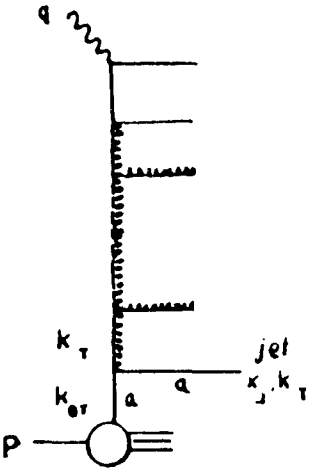

Figure 14. Diagrammatic representation of a deep inelastic event which contains an identified jet with longitudinal and transverse momenta x_{jp} and K_T respectively.

not to lie in the small x region and the transverse momentum at the gluon-parton vertex is so ordered that the exchanged gluon and the jet have approximately the same transverse momentum, since we chose events with $K_T^2 \sim Q^2$ the Q^2 evolution is also neutralised and attention is focussed on the small x or rather small $\frac{x}{x_j}$ behaviour.

The rate (or cross section) of deep inelastic events containing an identified jet is conveniently expressed as differential structure function in terms of the jet variables x_j and K_T [9].

$$x_j K_T^2 \frac{\partial F_2(x, Q^2, x_j, K_T^2)}{\partial x_j \partial K_T^2} \sim \alpha_s(K_T^2) x_j [g(x_j, K_T^2) + \frac{4}{9}\{q(x_j, K_T^2) + \bar{q}(x_j, K_T^2)\}] \cdot F(\frac{x}{x_j}, K_T^2, Q^2) \quad (37)$$

Where the factor F represent the photon-gluon process shown by the upper blob of Fig. (15) and $\frac{F}{K_T^2}$ is identified with the gluon structure function. $F(\frac{x}{x_j}, K_T^2, Q^2)$ satisfies the Lipatov equation with solution

$$F(\frac{x}{x_j}, K_T^2, Q^2) \sim \left(\frac{x}{x_j}\right)^{-\alpha_P + 1} \quad (38)$$

in the leading $\ln\left(\frac{x_j}{x}\right)$ approximation.

In Fig. (16), we plot $x_j \partial^2 F_2 / \partial x_j \partial K_T^2$ vs x_j taking cut off of $K_0^2 \approx 1\,\text{GeV}^2$ and the B set of the KMRS input [10]. The results are shown by the continuous curves as a function of x_j for different x and $K_T^2 \approx Q^2 \approx 5\,\text{GeV}^2$ and $K_T^2 = 10\,\text{GeV}^2$, $Q^2 \approx 5\,\text{GeV}^2$ respectively. In the same figure we also show (as a dashed curve) the prediction of the approximation without the Lipatov effect. An inspection of the figure shows that the difference is dramatic, particularly at small x ($x \leq 10^{-3}$, in the region around $x_j \sim 0.1 - 0.2$).

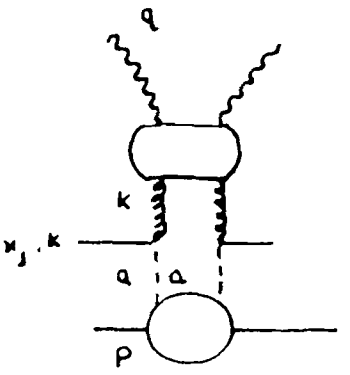

Figure 15. The diagram giving the cross section for deep inelastic scattering events containing an identified jet (x_{jp}, K_T).

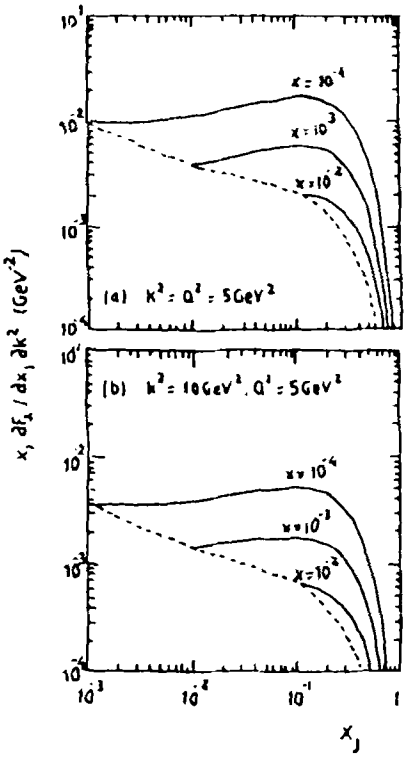

Figure 16. The differential structure function, Equation (37) for deep inelastic (x, Q^2) events with an identified jet (x_{jp}, K_T) as a function of x_j. The dashed curve corresponds to absence of Lipatov effect.

Thus the measurements of deep inelastic (x, Q^2) events accompanied by an identified jet (x_j, K_T^2) with $K_T^2 \approx Q^2$, will provide a unique way of investigating the Lipatov perturbative QCD growth expected at small (x/x_j). This QCD landmark measurement should be possible at HERA by studying the shape of the jet spectrum as a function of x and x_j in the region $x \sim 10^{-3}$ and $x_j \sim 0.1$.

7.3. Measurement of hot spots at HERA

As discussed earlier, there is a possibility that the "saturation" of soft gluons may set in non-uniformly, i.e. there may be regions inside the nucleon (Fig. 11) which are more densely populated by soft gluons than others. Since the structure function F_2 (total photon-hadron cross section) measures the parton density, averaged over the full size of the hadron, one needs to look at exclusive final states which measure the distribution of partons inside limited subregions of the hadron. Such an experiment is again the semi inclusive process where a jet (x_j, K_T^2) is observed. Here too $K_T^2 \leq Q^2$. Now $R^2_{Parton} \sim \frac{1}{Q^2}$, for the transverse radius of the parton struck by the photon and $R^2_{jet} \sim \frac{1}{K_T^2}$ is the square of the average transverse distance, by which the parent gluon of the jet is separated from this parton. If $K_T^2 \leq Q^2 \leq Q_0^2$, then

$$R^2_{Parton} \leq R^2_{jet} \ll R^2_{Hadron} \tag{39}$$

and this process explores the parton cloud of diameter R_{jet} around the struck parton.

The relevant double differential cross section has already been shown in (37), which contains the function $F(\frac{x}{x_j}, Q^2, K_T^2)$ satisfying the Lipatov equation:

$$F(Z, K_T^2, Q^2) = F_0(Z, K_T^2, Q^2) + \frac{3\alpha_s}{\pi} K_T^2 \int_Z^1 \frac{dZ'}{Z'} \int_0^\infty \frac{dK'^2}{K'^2} \left[\frac{F(Z', K'^2, Q^2) - F(Z, K_T^2, Q^2)}{|K'^2 - K_T^2|} + \frac{F(Z, K_T^2, Q^2)}{(4K'^4 + K_T^4)^{\frac{1}{2}}} \right]. \tag{40}$$

The soultion of (40) in the limit $(x/x_j) \rightarrow 0$ is given by (38). Any deviation from this would be indicative of "local saturation" i.e. of the existence of a "hot spot".

Bartels et al. [23] recently reported a further analysis on this topic. Their conclusion is: HERA should be able to find "hot spot" events. For a data sample corresponding to an integrated luminosity of O(10) pb^{-1}, one can expect a few 1000 potentially usable jets. Signals of new partonic interactions would manifest themselves in a cross section that lies below that of Fig. 16 since corrections to the Lipatov Pomeron are expected to come with a negative sign.

8. Summary

In the present talk, we have given an overview of low X physics. As noted in the text, the low x regime is a new frontier in perturbative QCD. It will also set in the transition from perturbative to non-perturbtive QCD. Starting from an intuitive parton basis, we have progressed through the relevant evolution equations and compared their predictions. We have pointed out the difficulties of distinguishing

them. It appears that the GLR equation needs further refinement [24] to make it quantitatively more viable. It is also pointed out that, to explore the new physics at low x, a study of structure functions is not sufficient; the study of semi inclusive phenomena is equally and even more important.

Let us conclude with an optimistic view that HERA and the forthcoming colliders will throw new light on low x physics.

Acknowledgements

I am grateful to Probir Roy for inviting me to deliver the present talk at the DAE symposium dedicated to the memory of the late P.K. Malhotra. I treasure his kindness shown to me during all these years. I also thank D.P. Roy for helpful communications.

References

[1] See for example F. Eisele, Nucl. Phys B (Proc. Suppl.) **18C** (1990) 1.

[2] See for example J. Bartels, Particle World **2** (1991) 46.

[3] V.N. Gribov and L.N. Lipatov, Sov. Jour. Nucl. Phys. **15** (1972) 438; **15** (1972) 675.

[4] G. Altarelli and G. Parisi, Nucl. Phys **B126** (1977) 297.

[5] L.V. Gribov, E.M. Levin and M.G. Ryskin, Phys. Rep. **100** (1982) 1.

[6] E. Reya in "Particle Phenomenology in the 90's", Ed. A. Datta, P. Ghosh and A Raychaudhuri (World Scientific 1992) 109.

[7] E.A. Kuraev, L.N. Lipatov and V.S. Fadin, Sov. Phys. JETP **45** (1977) 199; Ya. Ya. Balitsky and L.N. Lipatov, Sov. J. Nucl. Phys. **28** (1978) 822.

[8] A.H. Mueller, Nucl. Phys. (Proc. Suppl) **18C** (1991) 125.

[9] J. Kwiecinski, A.D. Martin and P.J. Sutton, Phys. Lett. **B287** (1992) 254; Phys Rev **D46** (1992) 921; and references therein.

[10] J. Kwiecinski, A.D. Martin, W.J. Stirling and R.G. Roberts Phys. Rev. **D42** (1990) 3645.

[11] J. G. Morfin and W.K. Tung, Fermilab-PUB-90/74.

[12] M. Gluck, E. Reya and A. Vogt, University of Dortmund Report Do-TH 91/7.

[13] A. Donnachie and P.V. Landshoff, Nucl. Phys. **B244** (1984) 322.

[14] P.V. Landshoff, Nucl. Phys (Proc. Suppl) **18C** (1991) 211.

[15] D. K. Choudhury and J.K. Sarma, Pramana - J. Phys. **38** (1992) 481; **39** (1992) 273.

[16] M. Areneodo et al., CERN - EP/89-121.

[17] D.K. Choudhury in " Plots, Quarks and strange particles", Proceedings of Dalitz Conference, 1990 Eds I.J.R. Aitchison, C/ H. Llewellyn smith and J.E. Paton (World Scientific, 1991) 194.

[18] E.M. Levin and M.G. Ryskin, Nucl. Phys B (Proc Suppl) **18C** (1990) 92.

[19] J. Bartels, J. Bhimlein and G.A. Scheler, Z Phys. **C50** (1991) 91.

[20] E. Eichten, I. Hinchliffe, K. Lane and C. Quigg, Rev. Modern Phys. **56** (1984) 579; Erratum **58** (1986) 1065.

[21] J.C. Collins and P.V. Landshoff, CERN - TH - 6300/91.

[22] A.H. Muller, J. Phys. **G17** (1991) 1443.

[23] J. Barter, A. De Roeck and M. Loewe, Z. Phys. **C54** (1992) 635.

[24] J. Bartels, Talk presented at the XXVI International Conference on High Energy Physics, Dallas, USA (1992);
E.M. Levin, DESY 92-122.

Discussion

R.S. Kaushal : Could you please throw some light on the physical significance of the nonlinear term in the evolution equation of BKFL type?

D.K. Chowdhury : The nonlinear term occurs in the GLR equation and not in BKFL. Its origin lies in the recombination of two parton chains. In usual GLAP evolution, it is absent since it deals with single parton chain.

D.K. Bhattacharjee : I would appreciate your comments on the increase in the number of partons, interactions between them and exponential rise of gluons within hadrons and the experimental support, if any, in relation to the evolution of proton structure function at low x.

D.K, Chowdhury : The exponential increase of gluons is in the prediction of GLAP evolution at low x. But such a rise cannot go on indefinitely as it violates unitarity. GLR equation, through its nonlinear term however, stops such a rise. Experimentally, of course, these features are yet to be tested.